Influence of plastic plasma on process of aluminium plasma jet formation

A. Kasperczuk[1], T. Pisarczyk[1], T. Chodukowski[1], Z. Kalinowska[1], S.Yu. Gus'kov[2], N.N. Demchenko[2], J. Ullschmied[3], E. Krousky[4], M. Pfeifer[4], K. Rohlena[4], J. Skala[4], and P. Pisarczyk[5]

[1]*Institute of Plasma Physics and Laser Microfusion, Warsaw, Poland*
[2] *P.N. Lebedev Physical Institute of RAS, Moscow, Russia*
[3]*Institute of Plasma Physics ASCR, v.v.i., Prague, Czech Republic*
[4]*Institute of Physics ASCR, v.v.i., Prague, Czech Republic*
[5]*Warsaw University of Technology, ICS, Warsaw, Poland*

1. Introduction

Supersonic laser-driven plasma jets attract attention of both astrophysicists [1-3] and laser plasma physicists [4], they are of interest also in developing new fast ignition concepts [5].
In 2006 we reported a simple method of plasma jet generation based on using a flat massive target with atomic number $Z \geq 29$ ($Z=29$ corresponds to Cu) irradiated by the third harmonic of a single partly defocused laser beam [6]. Our experiments at the Prague Asterix Laser System (PALS) laser facility [7] have proved that annular target irradiation plays a decisive role in the plasma jet forming [8]. However, this mechanism acts properly only in the case of heavy target materials. If the target is made of light materials like plastic (CH) or Al, no plasma jets are observed, in spite of that the initial laser intensity distribution is the same. However, our investigations of the plasma stream emitted from a joint of light and heavy target materials (Al-Cu or CH-Cu) [9] have shown that the plasma jet is not propagating normally to the target surface, but it is deflected to the side of the heavier material. The angles of jet deflection for Al-Cu and CH-Cu joints were about 5^o and 10^o, respectively. The theoretical analysis [10] allowed us to evaluate the average pressures in plastic and copper plasmas near the critical densities during the period of laser action. They are equal to 14.3 Mbar and 10.6 Mbar, respectively. The ratio of plastic and copper plasma pressures amounts to 1.35.

As both the experimental results and the theoretical analyses allowed us to conclude that the lighter is the plasma the higher is its pressure, so there was the question about possibility of the Al plasma jet creation using the plastic plasma as a compressor.

2. Experimental setup and conditions

The reported experiment was carried out with the use of the PALS iodine laser facility. The plasma was generated by a laser beam of diameter of 290 mm, which was focused by means of an aspheric lens with a focal length of 600 mm for the third harmonic of the laser radiation used (λ=0.438 μm). The following laser parameters have been chosen: laser energy 130 J, focal spot diameters (Φ_L) 800, 1000, and 1200 μm, and pulse duration 250 ps (full width at half maximum). The laser irradiated a plastic target with an Al cylindrical insert of 400 μm in diameter. To study the Al plasma stream propagation and its interaction with plastic plasma: a three-frame interferometric system was used.

3. Investigations of the Al plasma compression by the plastic plasma.

To ensure a predominance of the plastic plasma amount enough for the effective Al plasma compression we started our basic investigations with Φ_L=800 μm. Then, the focal spot diameter was gradually increased by 200 μm up to 1200 μm. The interferometric measurements have shown that the best result of the Al plasma compression corresponds to the maximum focal spot diameter. Therefore here we present and discuss the results

correspond only to Φ_L=1200 μm. In Fig. 1 the sequences of electron density distributions are presented.

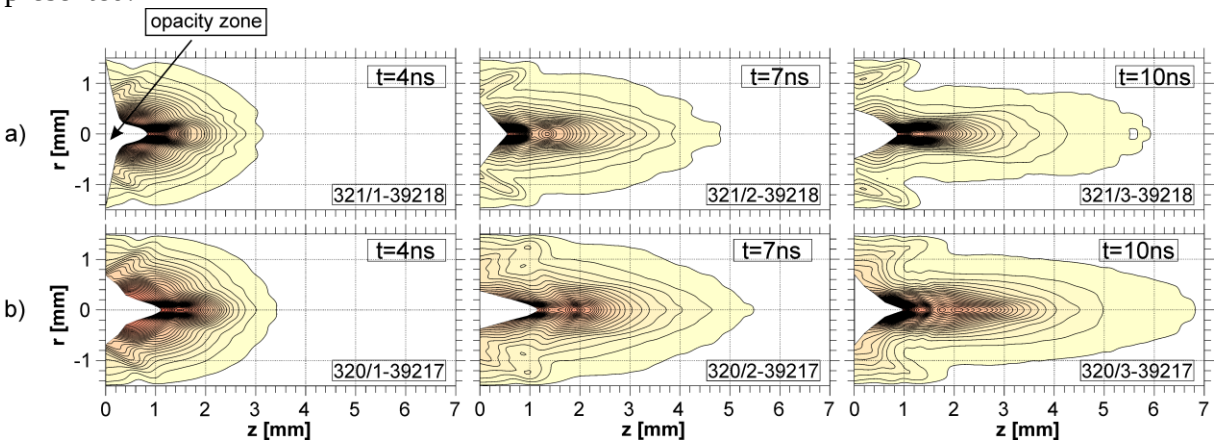

Fig. 1. The electron density distributions for the Al target (a) and the plastic target with the Al insert (b).

One can see great differences in the plasma configurations between the pure Al plasma (a) and the Al and plastic plasma composition (b) at t=10 ns. The former conserves its divergent structure in the observation period whereas the latter changes its initial divergent plasma expansion, becoming convergent.

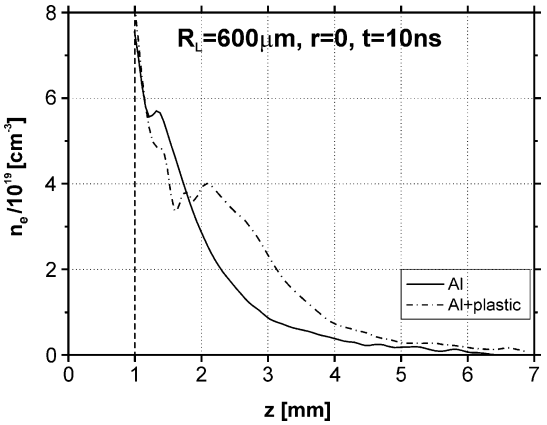

Fig. 2. Diagrams of the electron density distributions along the axis for the Al target and the plastic target with the Al insert.

In Fig. 2 diagrams of the electron density distributions along the axis for the Al target and the plastic target with the Al insert are drawn. As it is seen the Al plasma compression leads to an increase of the electron density at the axis for z > 2 mm by a factor of 2 in comparison with the electron density of plasma launched on the Al target.

However a life-time of this plasma configuration is relatively short. The interferograms recorded at later instants (t ≥ 10 ns) show that the compressed earlier plasma expands radially with a velocity of 2.7×10^7 cm/s (see Fig. 3). Of course, it leads to the electron density decrease at the axis.

Changes of the electron density at the axis

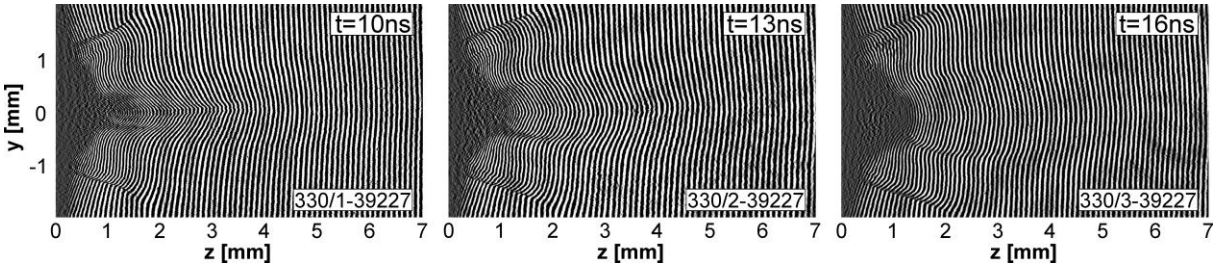

Fig. 3. Sequence of interferograms illustrative of the Al plasma jet expansion at later instants.

for both the target used versus time corresponding to z=2.1 mm, i.e. the electron density local maximum (see Fig. 2), are presented in Fig. 4. One can see that the Al plasma compression at this cross-section lasts about 10 ns. Later on, the electron density drops drastically below the value proper for the Al only plasma.

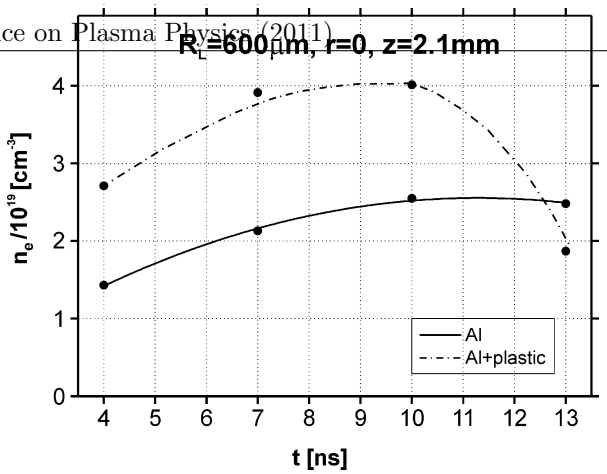

Fig. 4. Diagrams of the electron densities change vs. time for both the target used.

4. Theoretical analysis of the experimental results

In Ref. 11 it was demonstrated that at the same irradiation conditions of two targets, which differ in atomic number, the lighter one is characterized by smaller evaporated mass and its larger expansion velocity. According to this paper results, the ratio of evaporated masses of aluminium (Al) and plastic (CH), i.e. mass per irradiated surface unit in g/cm^2, can be estimated by the following formula:

$$\frac{\Delta m_{Al}}{\Delta m_{CH}} = \left(\frac{\chi_{Al}}{\chi_{CH}} \right)^{1/2} , \qquad (1)$$

where: $\chi = \kappa\rho / C_V$ - coefficient of thermal conductivity, ρ - initial target density, C_V – specific heat, κ - Spitzer's coefficient of electron heat conductivity expressed in the form:

$$\kappa = \frac{20(2/\pi)^{3/2} T_e^{5/2} Z^*}{m_e^{1/2} e^4 Z^{2*} \Lambda} \left(\frac{0.472 Z^*}{4 + Z^*} \right) \qquad (2)$$

here: T_e is the electron temperature, m_e and e are the mass and charge of the electron, respectively, Λ is Coulomb logarithm, Z^* and Z^{2*} are the charge and squared charge of ions averaged over the different types of ions. The estimation gives $\Delta m_{Al} / \Delta m_{CH}$ = 1.99. Because at later time the absorbed energy by plasma is completely transformed into the kinetic energy of plasma expansion, so $\Delta m (u^2)^* / 2 = E_a / S_f$, where $(u^2)^*$ - the square of plasma velocity averaged from the mass point of view, E_a – the absorbed energy, and S_f –surface of target irradiation. As a result, the estimation of the ratio of plastic and Al plasma expansion velocities gives the value $u^*_{CH} / u^*_{Al} = (\Delta m_{Al} / \Delta m_{CH})^{1/2}$ = 1.41. Here $u^* = \sqrt{(u^*)^2}$. However, the expansion velocity profiles of different materials have the same form, therefore the ratio of their velocity maximums has also the same value of 1.41. Since the plastic plasma overtakes the Al one, it induces an enhancement of the plastic plasma pressure beyond the pressure of Al plasma. It results in the plasma motion towards the axis. The two plasmas contact boundary is deflected from the normal to the target surface at certain angle α . This angle depends on a difference in initial densities of target materials used. For example, the boundary of CH-Cu plasmas is deflected by 10^o, whereas the boundary of Al-Cu plasmas – by 5^o. Combination of CH-Al, close to the case of Al-Cu from the density ratio point of view, should roughly give α=5^0. As the plasma motion is directed both along the axis z and toward the axis z (i.e. along the radius r), as a result, the Al plasma is focused at distance $z_f = R_{Al}/\mathrm{tg}\alpha$=2.3 mm, where R_{Al}=200 μm – initial radius of the Al insert. It corresponds to the diagram in Fig. 2. Evaporated masses of the CH and Al materials amount to: $\Delta m_{CH} = 2.4 \times 10^{-4}$ g/cm^2, and $\Delta m_{Al} = 4.78 \times 10^{-4}$ g/cm^2. It gives the average velocity of Al plasma (in the above mentioned sense) $u^*_{Al} = 2.19 \times 10^7$ cm/s. Because this velocity is characteristic for the whole evaporated mass, then the point at distance z=2.1 mm corresponds to the instant of 9.6 ns in

Fig. 4, i.e. when the plasma density reaches its maximum. So, the theoretical valuation is in accordance with the experimental result.

Now, let us estimate theoretically the growth of electron density of Al plasma at distance z_f=2.1 mm because of its radial compression so as to compare it with that given in Fig. 4. The plasma temperature in this area is about 100 eV. The electron densities without (for the Al target only) and with the radial compression are equal to $n_{e0}=2.5\times10^{19}$ cm^{-3} and $n_{e1}=4\times10^{19}$ cm^{-3}, respectively. When the process of plasma focusing is ended, the plasma reflection from the axis occurs and the plasma radial velocity changes its sign. An increase of this velocity amounts to $2u_r$, where $u_r=u^*_{Al}\times tg5^0=1.92\times10^6$ cm/s. To estimate the plasma momentum the following value is taken into consideration: $\Delta m_{rAl}=\rho_{Al}R_{Al}$, where ρ_{Al} – the Al plasma density corresponding to the electron density of Al plasma without compression (2.5×10^{19} cm^{-3}). The plasma momentum change takes place due to the pressure increase inside the compressed plasma area compared with the "undisturbed" pressure, when there is no radial compression. The time-averaged plasma pressure at the axis in the case of the radial compression can be estimated as $(p_1+p_0)/2$, where $p_1=p_0(\rho_1/\rho_0)^\gamma$. Due to the low plasma temperature the thermal conductivity is neglected. Difference in the plasma pressures $(p_1+p_0)/2- p_0=(p_1-p_0)/2$ leads to the plasma reflection from the axis. So, the equation for the plasma momentum can be written as follows:

$$2u_r\,\Delta m_{rAl}=\frac{p_0}{2}\left[\left(\frac{\rho_1}{\rho_0}\right)^\gamma-1\right]\Delta t\,, \tag{3}$$

where: $\Delta t=R_{Al}/c_s$, c_s =8.43×10^6 cm/s – sound speed. The equation (3) allows to get the compression value ρ_1/ρ_0 =1.7, which is close to the experimental value n_{e1}/n_{e0} = 1.6 at the instant of 10 ns, taken from Fig. 4.

5. Conclusions

In this work we have demonstrated possibility of the Al plasma jet creation using the plastic plasma as a compressor. In our experiments we took advantage of the fact that the lighter is the plasma, the higher is its pressure. On the basis of theoretical analysis one can conclude that difference in plasma pressure related to plasmas with different atomic numbers results from differences in their expansion features. The estimation of the ratio of plastic and Al plasma expansion velocities gives the value of 1.41. As a result, the plastic plasma overtakes the Al one. It induces an enhancement of the plastic plasma pressure beyond the pressure of Al plasma and, in consequence, the Al plasma motion towards the axis.

References

[1] D.D. Ryutov, R.P. Drake, and B.A. Remington, Astrophys. J. Supplement Series **127**, 465 (2000).

[2] P.M. Bellan, Phys. Plasmas **12**, 058301-1-8 (2005).

[3] B.A. Remington, R.P. Drake, and D.D. Ryutov, Rev. Modern Phys. **78**, 755 (2006).

[4] W. Hong, Y. He, T. Wen, H. Du, J. Teng, X. Qing, Z. Huang, W. Huang, H. Liu, X. Wang, X. Huang, Q. Zhu, Y. Ding, and H. Peng. Laser and Particle Beams **27**, 19 (2009).

[5] P. Velarde F. Ogando, S. Eliezer, Jm. Martinez-Val, J. M. Perlado, and M. Murakami. Laser Part. Beams **23,** 43 (2005).

[6] A. Kasperczuk, T. Pisarczyk, S. Borodziuk, J. Ullschmied, E. Krousky, K. Masek, K. Rohlena, J. Skala and H. Hora, Phys. Plasmas **13,** 062704-1 (2006).

[7] K. Jungwirth, A. Cejnarova, L. Juha, B. Kralikova, J. Krasa, E. Krousky, P. Krupickova, L. Laska, K. Masek, T. Mocek, M. Pfeifer, A. Prag, O. Renner, K. Rohlena, B. Rus, J. Skala, P. Straka, and J. Ullschmied, Phys. Plasmas **8**, 2495 (2001).

[8] A. Kasperczuk, T. Pisarczyk, M. Kalal, J. Ullschmied, E. Krousky, K. Masek, M. Pfeifer, K. Rohlena, J. Skala and P. Pisarczyk, Appl. Phys. Letter **94,** 081501 (2009).

[9] T. Pisarczyk, A. Kasperczuk, M. Kalal, S.Yu. Gus'kov, J. Ullschmied, E. Krousky, K. Masek, M. Pfeifer, K. Rohlena, J. Skala, and P. Pisarczyk, Proceedings of 35th EPS Conference on Plasma Phys., Hersonissos, 9- 13 June 2008, ECA Vol. 32, P- 1.118 (2008).

[10] A. Kasperczuk, T. Pisarczyk, J. Badziak, S. Borodziuk, T. Chodukowski, S.Yu. Gus'kov, N.N. Demchenko, J. Ullschmied, E. Krousky, K. Masek, M. Pfeifer, K. Rohlena, J. Skala, and P. Pisarczyk, Phys. Plasmas **17,** 114505-1 (2010).

[11] A. Kasperczuk, T. Pisarczyk, N.N. Demchenko, S.Yu. Gus'kov, M. Kalal, J. Ullschmied, E. Krousky, K. Masek, M. Pfeifer, K. Rohlena, J. Skala, and P. Pisarczyk, Laser and Particle Beams, **27**, 415 (2009).